Laser Light and Electrodes: Interaction Mechanisms and Electroanalytical Applications

Jennifer L. Brennan and Robert J. Forster*

National Centre for Sensor Research, School of Chemical Sciences, Dublin City University, Dublin 9, Ireland

Received: October 11, 2002; In Final Form: December 13, 2002

The effect of 355 nm, 10 ns laser pulses of 3−11 MW cm^{-2} intensity on gold macrodisk electrodes has been investigated. Repetitive pulsing increases the standard heterogeneous electron transfer rate constant, k°, for $Fe(CN)_6^{3-/4-}$ from $(9.2 \pm 0.3) \times 10^{-5}$ to $(2.4 \pm 0.1) \times 10^{-3}$ cm s^{-1}. The k° value becomes larger with increasing laser pulse intensity, and the enhancement is removed by conventional mechanical polishing. The effect of laser irradiation on the electrode surface has been investigated using scanning electron microscopy and by measuring the capacitance as well as the open circuit potential. These results suggest that the primary activation mechanism involves thermally driven desorption of adventitious surface impurities. The dependence of the laser-induced current−time transients on the applied potential has also been investigated. These transients do not exhibit the single exponential decay behavior expected if the laser pulse caused a simple change in the interfacial potential, e.g., through changes in the interfacial ion distribution. Rather, they are interpreted in terms of double layer charging at short times in response to a laser-induced change in the interfacial potential followed by a thermal diffusion process that depends on the applied potential. While the resistance is independent of the applied potential, the double layer capacitance of this interface that has been heated by the laser pulse to approximately 500 K shows a minimum at +0.100 V that is consistent with the potential of zero charge. The thermal conductivity and heat capacity depend strongly on the applied potential reaching maximum values at approximately +0.100 V of 3.19 J cm^{-1} K^{-1} and 0.13 J g^{-1} K^{-1}, respectively. The lower values observed at more extreme potentials are consistent with laser-induced heating of the interface and provide a powerful new insight into the potential dependence of heat conduction in metals.

Introduction

The in situ interaction of intense laser light pulses and electrode surfaces is of increasing importance for electroanalysis from both the practical perspective of generating surfaces that are activated toward electron transfer and as a method of elucidating the interfacial structure. For example, McCreery and co-workers have made pioneering contributions by using high intensity (10−80 MW cm^{-2}) pulses of 1064 nm light to activate the surface of glassy carbon,[1−3] highly ordered pyrolytic graphite (HOPG),[4] and platinum[5] electrodes. At these power densities, laser activation removes adsorbed contaminants and restructures the electrode material giving increased heterogeneous electron transfer rates to solution phase redox probes. Related experiments by Strein and Ewing[6] have shown that the reversibility of the cyclic voltammetry response for biological amines at carbon fiber microelectrodes can be significantly improved by treatment with pulses from a nitrogen laser prior to the voltammetric sweep. More aggressive laser treatments have also been developed. For example, Watanabe and co-workers[7] have utilized high-intensity pulses of infrared laser light to produce clean electrode surfaces by periodically ablating the top layer of a gold electrode surface during the potential sweep. This approach, known as *laser ablation voltammetry*, can cause significant damage to the electrode surface limiting the lifetime of the electrode. Compton et al.[8] have adapted this method and used lower intensity 532 nm light during the potential sweep, which causes less damage to the electrode surface. Using this *laser activation voltammetry* technique, they have obtained reproducible steady-state voltammograms at gold and platinum electrodes for analytes that are difficult to analyze by traditional electrochemical methods. The technique also allows electrochemistry to take place in passivating media, as the laser pulse periodically removes any material deposited on the electrode during electrochemical experiments.[9]

Beyond these electroanalytical applications, pulsed laser sources have been used to elucidate the structure of the electrode/solution interface, e.g., to study the electrical double layer on mercury[10,11] and platinum and gold single-crystal electrodes,[12−14] and, more recently, to probe the electrode kinetics of fast reactions.[15,16] The current transients obtained upon laser illumination are typically interpreted as arising from restoration of the double layer and adsorbed ions following perturbation by the laser. However, significant issues regarding the role of thermally driven polarization of the electron density within the metal and ion desorption, as well as the potential dependence of these temporal phenomena, remain outstanding.

Feldberg and co-workers[15,16] have developed an indirect laser induced temperature (ILIT) jump method that involves indirect irradiation of the electrode; i.e., the laser pulse impinges on the "back face" or nonelectrolyte electrode surface. In this method, some of the incident photons are absorbed by the thin foil or film electrode and thermalize virtually instantaneously, causing a rapid rise in the interfacial temperature. This process changes the open circuit potential as the system attempts to reestablish equilibrium under the new conditions. In contrast to classical charge injection methods, thermal perturbation does not cause a large *iR* spike, making data interpretation more straightforward. Moreover, the ILIT jump method offers the possibility of extracting information about thermal as well as electrochemical properties of electrodes and adsorbed layers.

* To whom correspondence should be addressed.

10.1021/jp027189g CCC: $25.00
Published on Web 08/05/2003

In this contribution, the effect of nanosecond pulse width 355 nm laser pulses of 3−11 MW cm^{-2} intensity on the surface and electrochemical properties of gold electrodes is presented. This wavelength is shorter than that previously investigated by other researchers and is close to the threshold for photoemission of electrons. Scanning electron microscopy has been used to probe the extent to which laser irradiation triggers structural changes of the electrode surface. When taken in conjunction with measurements of the double layer capacitance, the open circuit potential, and the heterogeneous electron transfer kinetics, an extensive insight into the mechanism of laser activation has been obtained. These investigations into improved electroanalytical performance have been complemented by investigations into the origin of the laser-induced current transients. These investigations provide a unique insight into the magnitude of the potential excursion induced by the laser pulse, the potential-dependent structure of the double layer and the potential-dependent thermal conductivity of gold.

Experimental Section

Apparatus and Materials. Potassium ferricyanide(III) (99.99%) and lithium perchlorate (99.9%) were purchased from Aldrich and were used without further purification.

Electrochemical cells were of conventional design. All potentials are quoted with respect to a CH Instruments Ag/AgCl reference electrode. Cyclic voltammetry, potential step chronoamperometry, and open circuit potential measurements were performed using a CH Instruments Model 660 electrochemical workstation and a conventional three-electrode cell, with a platinum flag functioning as counter electrode. The working electrode was a 2 mm diameter gold macrodisk (CH Instruments) and was polished using a slurry of 0.05 μm alumina and water on a felt pad before use. All solutions were degassed using nitrogen.

The light source used in these experiments was a Spectron Lasers Q-switched Nd:YAG laser with a 10 ns pulse width and 10 Hz repetition rate. The laser output was set to the third harmonic at 355 nm. At this wavelength the laser is capable of a power intensity output of between 3.19 and 11.01 MW cm^{-2}. Laser intensities were measured using a Spectron Instruments triple diode energy monitor No. 23 coupled to a Hewlett-Packard 54510A 250 MHz digitizing oscilloscope.

Laser activation was carried out for electrodes in air and in contact with a solution. Activation in air was carried out using a Safelab thermometer adapter (Aldrich) as an electrode holder and clamping it in a fixed position in front of the laser. The electrode may be easily positioned inside the adapter and removed following laser activation. For activation in solution, a cell was manufactured by drilling an electrode diameter sized hole in one wall of a poly(methyl methacrylate) disposable cuvette (Kartell). A watertight seal was achieved by fixing an O-ring over the hole in the cuvette wall with epoxy resin (Radionics) and surrounding the join with silicone sealant (Radionics). The cell was fixed in position in front of the laser by the use of a conventional stand and clamp arrangement.

The capacitance of gold macrodisk electrodes was determined by recording the current decay following the application of a 20 mV potential step across the electrode. The decay transients were analyzed in Microsoft Excel, and the capacitance of the electrode was obtained from the slope and intercept of the linearized current decay. The peak-to-peak separations of potassium ferricyanide(III) cyclic voltammograms, ΔE_p, were determined using the CHI 660 software, and the results were analyzed using Microsoft Excel. Heterogeneous electron transfer rate constants, k°, were calculated from ΔE_p values using the method of Nicholson[17] and by fitting the complete voltammogram using the simulation software of the CH Instruments Model 660 electrochemical workstation.

The effect of laser radiation on the capacitance, open circuit potential, and electron transfer kinetics of a gold macrodisk electrode was monitored as follows: after 10 min of mechanical polishing, the electrode was placed in a conventional electrochemical cell and the parameter of interest was recorded. The electrode was then removed from the electrochemical cell and placed in the laser activation cell. Where activation was carried out in solution, the cell was filled with Milli-Q water and approximately 3000 laser pulses were applied to the electrode surface. The electrode was then removed from the laser cell and returned to the electrochemical cell, where the parameter of interest was recorded.

In the measurement of laser current transients, a Hewlett-Packard HP8003A pulse generator was used to repetitively trigger the application of a fixed potential from a custom-built function generator−potentiostat to a two-electrode cell. A Stanford Research Instruments Model DG535 four channel digital pulse generator/delay generator was used as controller to simultaneously trigger the laser pulse and a Hewlett-Packard 54201A digitizing oscilloscope, which was used to monitor the applied potential and capture the current transients. The data were transferred to a PC using a National Instruments GPIB-232CT controller and were analyzed in Microsoft Excel. A Pt flag and an Ag/AgCl reference electrode were combined to form a counter electrode. The flag lowered the resistance and provided a high-frequency path. The supporting electrolyte throughout was 0.1 M $LiClO_4$.

Scanning electron microscopic images were obtained using a Hitachi S3000N scanning electron microscope.

Results and Discussion

Heterogeneous Electron Transfer Dynamics. The ferri/ferrocyanide couple is one of the most extensively investigated electron transfer reactions.[18] Recent investigations have shown that the redox process is not a simple outer sphere electron transfer but can involve a preassociated complex, leading to slow heterogeneous electron transfer kinetics at both glassy carbon[19] and metal electrodes.[20,21] These slow kinetics have been attributed to the formation of a Prussian Blue like passivating film during cyclic voltammetry[22,23] which is related to the surface properties of the electrode.[19,24] This sensitivity to the interfacial properties makes ferri/ferrocyanide a useful model system for investigating the effects of laser irradiation on electrode surfaces. Laser activation using 1064 and 532 nm light has previously been shown to enhance the rate of heterogeneous electron transfer to ferricyanide.[2,8] Here, the effect of 355 nm light on the heterogeneous electron transfer rate constant for ferricyanide has been studied as a function of the power density.

Figure 1 shows representative cyclic voltammograms of 5 mM ferricyanide before and after laser activation with a laser intensity of 11 MW cm^{-2}. The most striking feature of Figure 1 is the improved peak shape and reduced peak-to-peak separation, ΔE_p, following laser irradiation. This observation suggests that irradiation of the electrode surface with the pulsed laser increases the rate of heterogeneous electron transfer across the electrode/solution interface. To quantify the extent of this increase, the complete voltammogram under semi-infinite linear diffusion conditions has been simulated using the Butler−Volmer formulation of electrode kinetics. Figure 1 reveals that the simulated voltammogram accurately reproduces the experi-

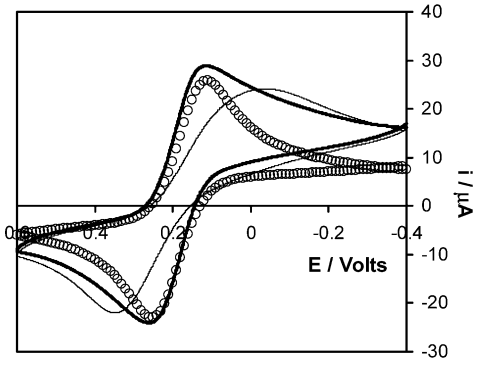

Figure 1. Cyclic voltammograms of 5 mM potassium ferricyanide recorded at a 2 mm diameter gold macrodisk electrode before (thin line) and after (thick line) laser activation with 3000 laser pulses of 355 nm, 11 MW cm^{-2} intensity laser light. Laser activation was carried out in Milli-Q water. The open circles represent the best fit voltammogram to the laser-activated response generated using the Butler−Volmer formulation of electrode kinetics assuming that the response is under semi-infinite linear diffusion control. The best-fit standard heterogeneous electron transfer rate constant is 2.4×10^{-3} cm s^{-1}. Cathodic currents are up and anodic currents are down. Scan rate is 100 mV s^{-1}. The supporting electrolyte is 0.1 M $LiClO_4$.

mental response observed following laser activation, indicating that the electron transfer mechanism involves simple heterogeneous electron transfer under semi-infinite linear diffusion conditions. The best-fit standard heterogeneous electron transfer rate constant, $k°$, obtained for the activated surface is $(2.4 \pm 0.1) \times 10^{-3}$ cm s^{-1}. This $k°$ is significantly larger than the value of $(9.2 \pm 0.5) \times 10^{-5}$ cm s^{-1} observed for an electrode immediately following mechanical polishing. This result is consistent with previous reports that demonstrated the feasibility of using pulses of high-intensity laser light to enhance the electrode kinetics of ferricyanide.[2,4,5,25] However, an important objective is to use low intensities so as to minimize physical damage to the electrode surface. Therefore, this investigation has focused on laser power densities between 3 and 11 MW cm^{-2} compared to the 10−100 MW cm^{-2} reported by other workers. To accurately probe the effect of laser pulse intensity on the electron transfer dynamics, it is essential to be able to restore the electrode surface to its nonactivated state, e.g., by polishing, between laser activation steps.

Figure 2 illustrates the change in standard heterogeneous electron transfer rate constant when an electrode that has been laser activated at a systematically varying laser intensity is mechanically repolished. This figure shows that, irrespective of the laser power, mechanical polishing restores the $k°$ value to a constant value of $(9.1 \pm 1.8) \times 10^{-5}$ cm s^{-1}, thus facilitating investigations into the correlation of $k°$ and the laser power.

Figure 3 illustrates the dependence of ΔE_p and $k°$ on the intensity of the laser pulses used for electrode activation. It shows clearly that the standard rate constant for heterogeneous electron transfer increases as the intensity of the laser radiation is sequentially increased. One possible mechanism of electrode activation is that the laser energy must be above a critical threshold for the desorption of adventitious impurities. Under these circumstances, one would expect a sigmoidal dependence of $k°$ on the laser intensity with high energy pulses being capable of rapid cleaning of the electrode surface, making $k°$ independent of the laser power above the threshold value. Alternatively, it is possible that an increasing laser energy progressively cleans the electrode surface, leading to a systematic increase in $k°$ with increasing laser energy over a wide range. The current data do not allow a definitive conclusion as to the appropriate mechanism to be drawn primarily because of the lack of data at laser

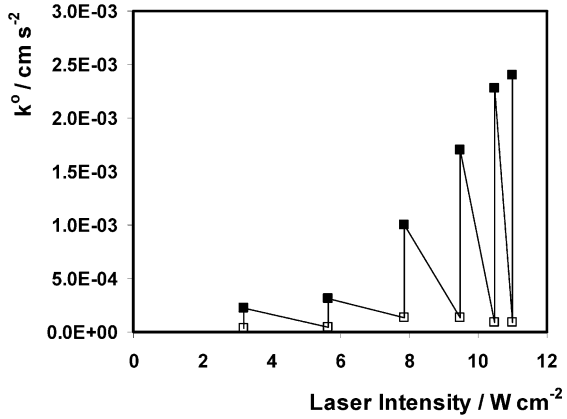

Figure 2. Effect of laser activation and subsequent mechanical repolishing of a gold electrode on $k°$ value for ferricyanide. Laser activation involves delivering approximately 3000 pulses of 355 nm laser light of increasing intensity to the gold electrode surface immersed in Milli-Q water (filled squares). Between laser activations, the electrode surface is renewed by conventional polishing on a felt pad with 0.05 μm alumina between the activation steps (open squares).

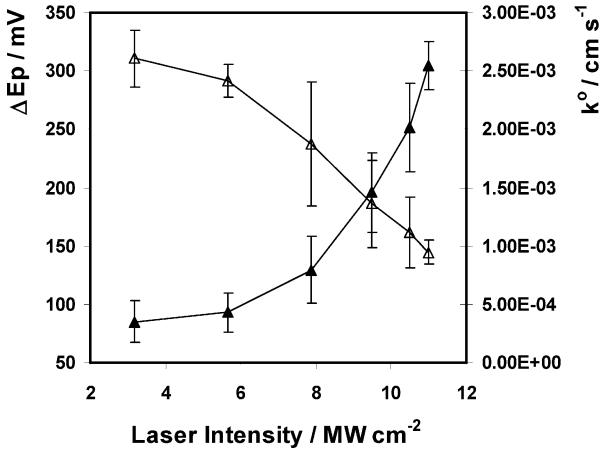

Figure 3. Effect of increasing 355 nm laser intensity on peak-to-peak separation (open triangles, left axis) and heterogeneous electron transfer rate constant (filled triangles, right axis) for 5 mM potassium ferricyanide. The supporting electrolyte is 0.1 M $LiClO_4$. Laser activation involves delivering approximately 3000 pulses of 355 nm laser light of increasing intensity to the gold electrode surface immersed in Milli-Q water.

powers above 11 MWcm^{-2} where ablation of the electrode tends to occur. However, the $k°$ values appear to be leveling off for laser intensities above 10 MW cm^{-2}, suggesting that the mechanism may involve a threshold laser power for desorption of impurities.[2,8,25]

Influence of Laser Pulsing on Interfacial Properties. Electrochemical measurements can provide a rapid and sensitive insight into the properties of the electrode surface. For example, the double layer capacitance, C_{dl}, is extremely sensitive to the composition and structure of the interfacial region and, being an extensive property, depends on the electrode area. Therefore, monitoring C_{dl} before and after laser activation provides an insight into changes in the interfacial structure and electrode area due to laser ablation. In contrast, the open circuit potential, OCP, of the electrode is an intensive property and is sensitive to the physicochemical properties, e.g., ablation, of the electrode surface.[26] Figure 4 demonstrates that increasing the intensity of the light applied to the gold electrode increases both the capacitance and the OCP. As capacitance is affected by both the surface area and cleanliness of the electrode, the effect of the laser activation could arise from a change in one or both

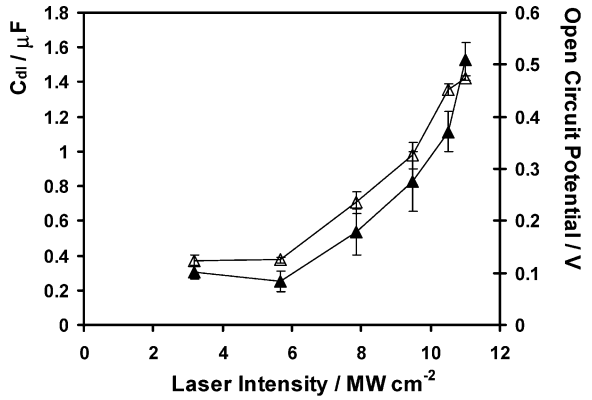

Figure 4. Effect of increasing 355 nm laser intensity on interfacial capacitance (filled triangles, left axis) and open circuit potential (open triangles, right axis) of a 2 mm diameter gold electrode. Laser activation involves delivering approximately 3000 pulses of 355 nm laser light of increasing intensity to the gold electrode surface immersed in Milli-Q water.

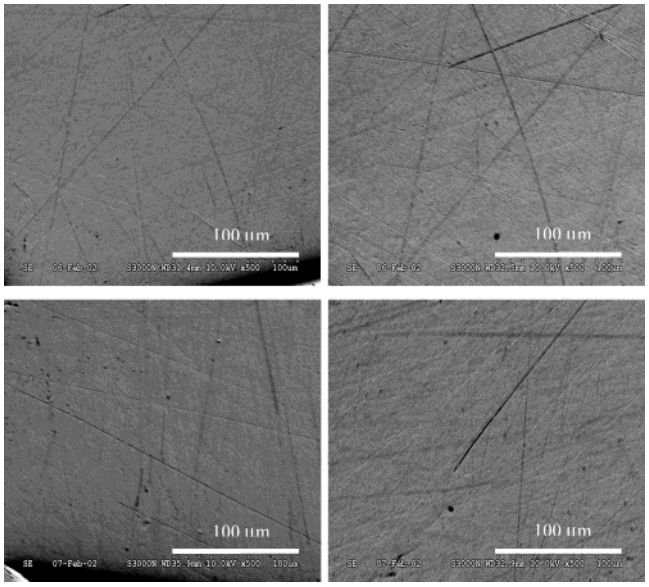

Figure 5. Scanning electron micrographs at a magnification of 280 (before reduction) of the surface of a 2 mm diameter gold disk electrode following, clockwise from top left, 10 min of conventional polishing with 0.05 μm alumina on a felt pad, and activation with 3000 pulses of 355 nm laser radiation of 5.7, 9.1, and 11.0 MW cm^{-2} intensity, respectively. All laser activation was carried out in aqueous 0.1 M $LiClO_4$. The electrode was repolished for 10 min between laser activations.

parameters. However, as OCP is primarily affected by surface composition, the OCP results tend to suggest that the most significant effect of the laser activation is removal of adsorbed debris from the electrode surface.

A more direct insight into the effect of laser activation on surface properties can be obtained by imaging the surface using scanning electron microscopy. Hinoue et al. have demonstrated that while intense laser pulses, of the order of 350 MW cm^{-2}, can efficiently activate the electrode kinetics of the ferri/ferrocyanide reaction at gold electrodes,[27] they result in substantial physical damage to the electrode surface. One potential advantage of using lower laser power densities of the kind explored here is that physical damage to the electrode surface ought to be minimized. Figure 5 illustrates scanning electron microscopic images of electrodes activated using 3000 laser pulses of power densities between 5.7 and 11.0 MW cm^{-2}. For this range of powers, laser pulsing appears to cause minimal

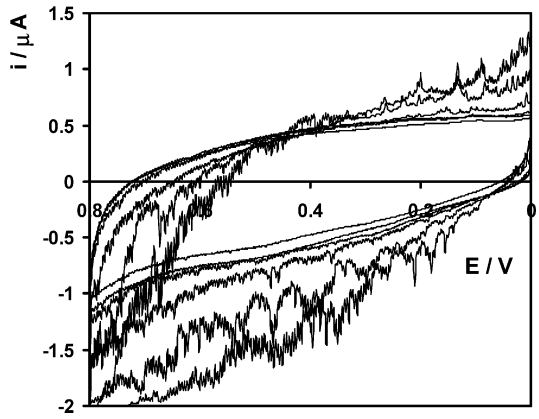

Figure 6. Cyclic voltammograms (CVs) of a 2 mm diameter gold electrode recorded during the application of laser pulses of increasing intensity. The innermost CV is for the minimum laser intensity (3.2 MW cm^{-2}), and the outermost CV is for the maximum intensity (11.0 MW cm^{-2}). The scan rate is 50 mV s^{-1}.

damage to the electrode surface, suggesting that the changes in OCP and capacitance observed are caused by the removal of adsorbed impurities.

Laser-Induced Current Transients. Figure 6 illustrates the effect of laser pulsing on the cyclic voltammetry of a 2 mm diameter gold electrode immersed in an aqueous 0.1 M $LiClO_4$ solution. Laser pulsing triggers small current "spikes" that are coincident in time with the laser pulse impinging on the electrode surface. These spikes increase in amplitude as the applied laser intensity is increased. Figure 6 also indicates that the amplitude of the spikes depends on the applied potential with only minor laser-induced current transients being observed close to 0.000 V. However, to obtain the time-resolved information necessary to achieve an insight into the nature of the current response triggered by a laser pulse, time-resolved chronoamperometry is required.

Theory and experiment have demonstrated that an impinging laser pulse causes the electrode surface to heat rapidly, e.g., by up to 250 K within 10 ns for the highest laser powers considered here. Therefore, to accurately record the current−time response associated with both rapid electrode heating and slower cooling, high-speed electrochemical instrumentation capable of accurately measuring current responses at nanosecond time scale has been used. Figure 7 illustrates laser-induced current transients. In this system, cathodic currents are positive and anodic currents are negative. Consistent with previous investigations by Compton and co-workers on polycrystalline gold in contact with 0.01 M $HClO_4$ as supporting electrolyte,[12] the largest transient is obtained at −0.700 V applied potential and the transients decrease in size as the applied potential is made more positive, eventually reaching zero amplitude at approximately +0.200 V, the potential of zero response. For potentials more positive than +0.2 V, a significant anodic laser-induced current transient is observed. Impinging a laser pulse on an electrode causes rapid heating of the surface followed by a relatively slower cooling process. According to Benderskii and co-workers,[28] this rapid change in the interfacial temperature is given by

$$\Delta T_m = \frac{2(1-R)q}{\sqrt{\pi\kappa c d} + \sqrt{\pi\kappa_{soln} c_{soln} d_{soln}}}\sqrt{t_0} \qquad (1)$$

where κ, c, d, and κ_{soln}, c_{soln}, and d_{soln} are the thermal conductivity, thermal capacity, and density of gold and the aqueous electrolyte solution, respectively, q is the power density

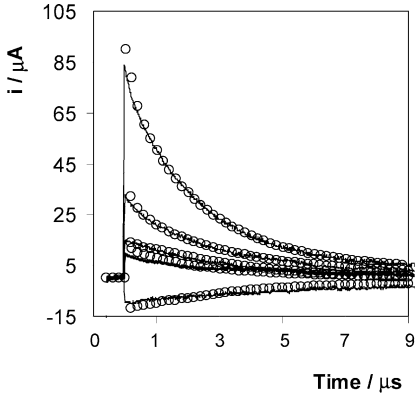

Figure 7. Laser-induced current transients observed following application of a 355 nm, 11 MW cm^{-2} intensity laser pulse to a 2 mm diameter gold disk electrode in aqueous 0.1 M $LiClO_4$, as a function of applied potential. From top to bottom, the applied potential was −700, −200, −100, and +600 mV, respectively. The open circles are the best fits of the experimental data to eq 4 that models the current−time transient in terms of double layer charging at short times and a slower cooling response at longer times.

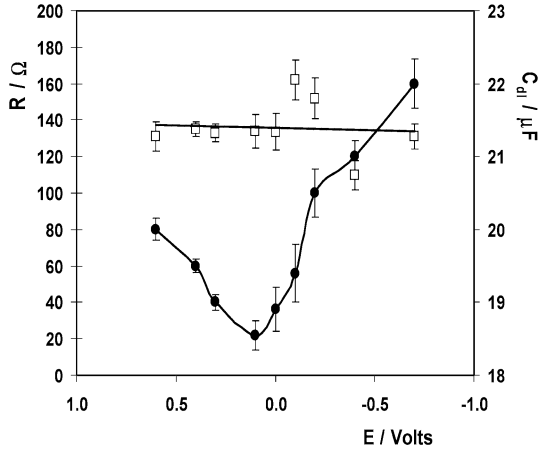

Figure 8. Potential dependence of total cell resistance, R (open squares, left axis), and capacitance, C_{dl} (filled circles, right axis), as determined by modeling the short time scale response of the laser-induced current transient induced by a 10 ns pulse of 355 nm laser light at a power density of 11 MW cm^{-2}.

of the laser at the surface which is assumed to be reduced from the actual laser power density by the reflectivity, R, of the gold surface at 355 nm (0.387), and t_0 is the laser pulse width, i.e., 10 ns.

As expressed within the Gouy−Chapman−Stern model of the electrochemical double layer, the double layer capacitance, C_{dl}, is expected to *decrease* with an *increase* in the interfacial temperature. Therefore, one might expect that the short time scale current response would be dominated by capacitive current, $i_C(t)$, arising from the virtually instantaneous thermally driven restructuring of the double layer. Under these circumstances, the short time scale current−time response can be analyzed according to[29]

$$i_C(t) = (\Delta E/R)\exp\left(-\frac{t}{RC_{dl}}\right) \quad (2)$$

where ΔE is the thermally driven change in the interfacial potential and R is the total cell resistance.

The change in the interfacial potential is related to the interfacial entropy of formation of the interface, ΔS_{form}, according to the electrocapillary equation:

$$\frac{\partial E}{\partial T} = -\left(\frac{\partial \Delta S}{q}\right)_T \quad (3)$$

The longer time scale current decay then corresponds to the slower cooling response and is given by[28]

$$\Delta T_m = \frac{2(1-R)q}{\sqrt{\pi\kappa cd} + \sqrt{\pi\kappa_{soln}c_{soln}d_{soln}}}[\sqrt{t-\sqrt{t-t_0}}] \quad (4)$$

Therefore, by combining eqs 2 and 4, it ought to be possible to fit the complete current−time transient. Analysis of this kind is important for the following reasons. First, it can provide an insight into the mechanism of laser activation of electrodes toward heterogeneous electron transfer that is useful for electroanalysis. Second, an insight into double layer structure can be obtained. Third, the potential dependence of the thermal conductivity and capacity of metals can be probed by investigating the dependence of the laser-induced current transients on the applied potential.

Figure 7 illustrates the best fits to the experimental data obtained by combining eqs 2 and 4, where κ, c, ΔE, R, and C_{dl} are freely adjustable parameters. The quality of the fit is excellent with the combination model accurately reproducing the current−time transients for all values of the applied potential investigated. An important test of the validity of this approach is to probe whether it accurately predicts the expected decrease in C_{dl} at higher temperatures, as well as the potential dependence of C_{dl} and R. Figure 8 illustrates the potential dependence of C_{dl} and R extracted using the combination model. For all potentials investigated, the interfacial capacitance is approximately 50% lower than that determined using conventional potential step chronoamperometry at room temperature. This decrease in C_{dl} is consistent with theory in that C_{dl} is expected to decrease with increasing temperature, and eq 1 predicts an increase in the interfacial temperature of approximately 250 K immediately after the 10 ns laser pulse with a power density of 11 MW cm^{-2}. Moreover, consistent with theory and experimental measurements, a minimum C_{dl} value is observed at approximately +0.2 V, which is in close agreement with the potential of zero charge, PZC, of gold. Also, the total cell resistance, 135 ± 14 Ω, is independent of the applied potential, and is consistent with that found using small-amplitude potential step chronoamperometry, 150 ± 10 Ω. As shown in Table 1, the change in the interfacial potential induced by the laser pulse, ΔE, depends on the applied potential with values between 8 and 1 mV being observed at −0.700 and +0.600 V. These values are entirely consistent with those reported by Compton for single-crystal gold[12] and platinum[13,14] using a coulostatic potential transient approach further supporting the use of eqs 2 and 4 to model the current transients. The absolute magnitude of C_{dl} and R, as well as their potential dependences, strongly suggests that it is appropriate to model the short time scale current response according to eq 2 and that laser-induced current transients can provide an insight into the properties of interfaces at temperatures that are not accessible using other approaches.

Figure 9 shows the potential dependence of the thermal conductivity and thermal capacity. It is important to note that despite the fact that κ and c are freely adjustable variables within the model, the best fit is obtained with values that are close to literature values for gold at room temperature, 3.15 J cm^{-1} K^{-1} and 0.129 J g^{-1} K^{-1}, respectively.[30] This close agreement suggests that eq 4 provides an appropriate description of the longer time scale current decay and arises in part because of thermally driven double layer restructuring as the electrode

TABLE 1: Potential Dependence of Laser-Induced Potential Excursion, ΔE, Total Cell Resistance, R, Double Layer Capacitance, C_{dl}, Gold Thermal Conductivity, κ, Thermal Capacity, c, and Thermal Diffusion Coefficient, D_T, as Determined by Fitting Laser-Induced Current Transients to a Combination Double Layer Charging and Thermal Relaxation Model[a]

E [V]	ΔE [mV]	R [Ω]	C_{dl} [μF cm^{-2}]	κ [J cm^{-1} s^{-1} K^{-1}]	c [J g^{-1} K^{-1}]	D_T [cm^2 s^{-1}]
−0.700	7.9	131 (7)	22.0 (0.3)	2.17 (0.04)	0.09 (0.002)	1.263 (0.05)
−0.400	5.3	110 (8)	21.0 (0.2)	2.01 (0.14)	0.08 (0.001)	1.263 (0.08)
−0.200	3.3	152 (11)	20.5 (0.3)	2.44 (0.05)	0.10 (0.002)	1.264 (0.05)
−0.100	3.2	162 (11)	19.4 (0.4)	2.44 (0.05)	0.10 (0.001)	1.264 (0.04)
0.000	1.3	133 (10)	18.9 (0.3)	3.19 (0.13)	0.13 (0.004)	1.267 (0.09)
0.100	1.3	134 (9)	18.6 (0.2)	3.19 (0.06)	0.13 (0.001)	1.267 (0.08)
0.300		133 (5)	19.0 (0.1)	2.55 (0.03)	0.10 (0.001)	1.270 (0.09)
0.400		135 (4)	19.5 (0.1)	2.00 (0.06)	0.08 (0.006)	1.271 (0.05)
0.600	1.2	131 (8)	20.0 (0.2)	1.67 (0.05)	0.07	1.272 (0.02)

[a] Values in parentheses are the errors determined by fitting at least three independent laser-induced current transients.

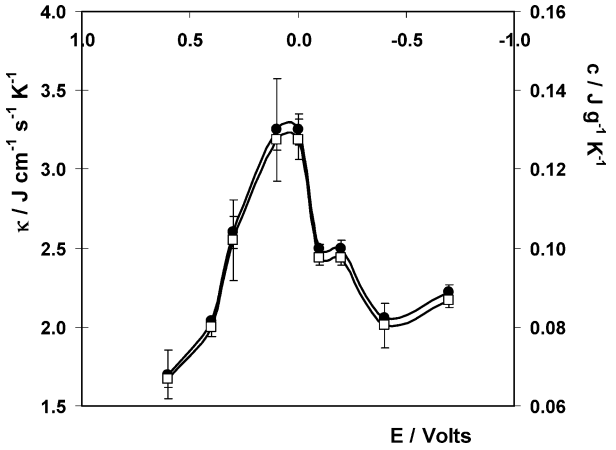

Figure 9. Potential dependence of thermal conductivity, κ (open squares, left axis), and thermal capacity, c (filled circles, right axis), for gold as determined by modeling the long time scale response of the laser-induced current transient induced by a 10 ns pulse of 355 nm laser light at a power density of 11 MW cm^{-2}.

cools. However, Figure 9 provides an insight into the potential dependence of the thermal properties of the metal side of the gold/solution interface. Both κ and c show marked potential dependence with the maximum values being observed at approximately +0.1 V and with lower values being observed for more positive or negative potentials. Differences in the reflectivity of the electrode surface caused by changing the applied potential would cause the temperature change induced by the laser pulse to depend on the applied potential, thus making κ and c appear to be potential dependent. However, given that κ is expected to decrease with increasing temperature while c is expected to increase, the observation in Figure 9 that the potential dependence of κ and c is indistinguishable strongly suggests that potential-dependent changes in electrode reflectivity are not the origin of the observed behavior. For all potentials investigated, the thermal diffusion coefficient is 1.26 ± 0.10, which is smaller than the literature value for gold at 298 K, i.e., 1.314 cm^2 s^{-1}. Given that D_T decreases with increasing temperature, this result is consistent with heating of the interface. The thermal diffusion coefficient obtained at the potential of zero response, 1.264 cm^2 s^{-1}, has been used to estimate the interfacial temperature as approximately 490 K immediately following the 10 ns laser pulse. An important test of internal consistency is to compare this value with that predicted by the Benderskii model. Equation 1 predicts that for a 10 ns laser pulse with a laser power density of 11 MW cm^{-2} the interfacial temperature will rise to approximately 520 K. Given the approximations involved in both of these approaches, the agreement between the predicted interfacial temperatures is satisfactory.

Conclusions

Gold electrodes, activated by applying repeated pulses of 355 nm, 10 ns laser pulses of power densities between 3 and 11 MW cm^{-2}, exhibit enhanced rates of heterogeneous electron transfer for ferrocyanide reduction. The rate of electron transfer can be increased by up to 2 orders of magnitude with the extent of the increase depending on the intensity of the laser pulses applied. Significantly, these improved electron transfer dynamics are removed by conventional polishing with a slurry of alumina and water on a felt pad. Measurements of the interfacial capacitance, open circuit potential, and scanning electron microscopic images of the electrode surface suggest that activation involves removal of adventitious adsorbates.

A model has been assembled that describes the laser-induced current−time transients in terms of a short time scale capacitive response driven by laser heating of the interface followed by a slower cooling process. Consistent with expectations, the total cell resistance determined from the short time scale component of these laser transients is independent of the applied potential and their magnitude is entirely consistent with independent potential step measurements at room temperature. In contrast, the double layer capacitance shows the classical minimum close to the potential of zero charge, providing an insight into the double layer structure at approximately 500 K. The model also allows the thermal conductivity and heat capacity to be determined. The potential dependence of these parameters has provided a new insight into the effects of electron energy and velocity on heat conduction through metal.

Acknowledgment. Financial support from Enterprise Ireland, the Irish Science and Technology Agency, and Ireland's Higher Education Authority under the Program for Research in Third Level Institutions is gratefully acknowledged.

References and Notes

(1) Hershenhart, E.; McCreery, R. L.; Knight, R. D. *Anal. Chem.* **1984**, *56*, 2256.
(2) Rice, R. J.; Pontikos, N. M.; McCreery, R. L. *J. Am. Chem. Soc.* **1990**, *112*, 4617.
(3) Jaworski, R. K.; McCreery, R. L. *J. Electrochem. Soc.* **1993**, *140*, 1360.
(4) Bowling, R. J.; Packard, R. T.; McCreery, R. L. *J. Am. Chem. Soc.* **1989**, *111*, 1217.
(5) Huang, W.; McCreery, R. L. *J. Electroanal. Chem.* **1992**, *326*, 1.
(6) Strein, T. G.; Ewing, A. G. *Anal. Chem.* **1991**, *63*, 194.
(7) Hinoue, T.; Kuwamoto, N.; Watanabe, I. *J. Electroanal. Chem.* **1999**, *466*, 31.
(8) Akkermans, R. P.; Suárez, M. F.; Roberts, S. L.; Fulian, Q.; Compton, R. G. *Electroanalysis* **1999**, *11*, 1192.
(9) Fulian, Q.; Compton, R. G. *Anal. Chem.* **2000**, *72*, 1830.
(10) Barker, G. C.; Cloke, G. *J. Electroanal. Chem.* **1970**, *52*, 568.
(11) Benderskii, V. A.; Velichko, G. I.; Kreitus, I. V. *J. Electroanal. Chem.* **1984**, *181*, 1.

(12) Climent, V.; Coles, B. A.; Compton, R. G. *J. Phys. Chem. B* **2001**, *105*, 10669.
(13) Climent, V.; Coles, B. A.; Compton, R. G. *J. Phys. Chem. B* **2002**, *106*, 5258.
(14) Climent, V.; Coles, B. A.; Compton, R. G. *J. Phys. Chem. B* **2002**, *106*, 5988.
(15) Smalley, J. F.; Krishnan, C. V.; Goldman, M.; Feldberg, S. W. *J. Electroanal. Chem.* **1988**, *248*, 255.
(16) Smalley, J. F.; Feldberg, S. W.; Chidsey, C. D.; Linford, M. R.; Newton, M. D.; Liu, Y. P. *J. Phys. Chem.* **1995**, *99*, 13141.
(17) Nicholson, R. S. *Anal. Chem.* **1965**, *37*, 1351.
(18) Peter, L. M.; Durr, W.; Bindra, P.; Gerischer, H. *J. Electroanal. Chem.* **1976**, *71*, 31.
(19) Wightman, R. M.; Deakin, M. R.; Kovach, P. M.; Kuhr, W. G.; Stutts, K. J. *J. Electrochem. Soc.* **1984**, *131*, 1579.
(20) Winkler, K. *J. Electronanal. Chem.* **1995**, *388*, 151.
(21) Iwasaki, Y.; Horiuchi, T.; Morita, M.; Niwa, O. *Surf. Sci.* **1999**, *427*−*428*, 195.
(22) Wieckowski, A.; Szklarczyk, M. *J. Electroanal. Chem.* **1982**, *142*, 157.
(23) Kawaik, J.; Kulesza, P. J.; Galus, Z. *J. Electroanal. Chem.* **1987**, *226*, 305.
(24) Goldstein, E. L.; Van de Mark, M. R. *Electrochim. Acta* **1982**, *27*, 1079.
(25) Poon, M.; McCreery, R. L. *Anal. Chem.* **1986**, *58*, 2745.
(26) Parsons, R. *Chem. Rev.* **1990**, *90*, 813.
(27) Hinoue, T.; Watanabe, I.; Watari, H. *Chem. Lett.* **1996**, 329.
(28) Benderskii, V. A.; Efimov, I. O.; Krivenko, A. G. *J. Electroanal. Chem.* **1991**, *315*, 29.
(29) Bard, A. J.; Faulkner, L. R. *Electrochemical Methods*—*Fundamentals and Applications*, 2nd ed.; Wiley: New York, 2001.
(30) *Handbook of Chemistry and Physics*, 75th ed.; Lide; D. R., Ed.; CRC Press: Boca Raton, FL, 1996.